Fiber-based cryogenic and time-resolved spectroscopy of PbS quantum dots

Matthew T. Rakher,[1,*] **Ranojoy Bose,**[2,3] **Chee Wei Wong,**[2] **and Kartik Srinivasan**[1]

[1]*Center for Nanoscale Science and Technology, National Institute of Standards and Technology, Gaithersburg, Maryland 20899-6203, USA*
[2]*Optical Nanostructures Laboratory, Center for Integrated Science and Engineering, Solid-State Science and Engineering and Mechanical Engineering, Columbia University, New York, New York 10027, USA*
[3]*Current Address: Institute for Research in Electronics and Applied Physics, University of Maryland, College Park, Maryland 20742, USA*

[*]matthew.rakher@gmail.com

Abstract: PbS quantum dots are promising active emitters for use with high-quality Si nanophotonic devices in the telecommunications-band. Measurements of low quantum dot densities are limited both because of low fluorescence levels and the challenges of single photon detection at these wavelengths. Here, we report on methods using a fiber taper waveguide to efficiently extract PbS quantum dot photoluminescence. Temperature dependent ensemble measurements reveal an increase in emitted photons concomitant with an increase in excited-state lifetime from 58.9 ns at 293 K to 657 ns at 40 K. Measurements are also performed on quantum dots on high-Q ($> 10^5$) microdisks using cavity-resonant, pulsed excitation.

© 2011 Optical Society of America

References and links

1. F. Wise, "Lead salt quantum dots: the limit of strong quantum confinement," Acc. Chem. Res. **33**, 773–780 (2000).
2. Y. Takahashi, Y. Tanaka, H. Hagino, T. Sugiya, Y. Sato, T. Asano, and S. Noda, "Design and demonstration of high-Q photonic heterostructure nanocavities suitable for integration," Opt. Express **17**, 18093–18102 (2009).
3. K. Srinivasan, P. E. Barclay, M. Borselli, and O. Painter, "Optical-fiber-based measurement of an ultrasmall volume, high-Q photonic crystal microcavity," Phys. Rev. B **70**, 081306R (2004).
4. S. Strauf, K. Hennessy, M. T. Rakher, Y.-S. Choi, A. Badolato, L. C. Andreani, E. L. Hu, P. M. Petroff, and D. Bouwmeester, "Self-tuned quantum dot gain in photonic crystal lasers," Phys. Rev. Lett. **96**, 127404 (2006).
5. J. Raimond, M. Brune, and S. Haroche, "Manipulating quantum entanglement with atoms and photons in a cavity," Rev. Mod. Phys. **73**, 565–582 (2001).
6. K. Srinivasan and O. Painter, "Linear and nonlinear optical spectroscopy of a strongly coupled microdisk-quantum dot system," Nature **450**, 862–865 (2007).
7. M. T. Rakher, N. G. Stoltz, L. A. Coldren, P. M. Petroff, and D. Bouwmeester, "Externally mode-matched cavity quantum electrodynamics with charge-tunable quantum dots," Phys. Rev. Lett. **102**, 097403 (2009).
8. C. Michael, K. Srinivasan, T. Johnson, O. Painter, K. Lee, K. Hennessy, H. Kim, and E. Hu, "Wavelength- and material-dependent absorption in GaAs and AlGaAs microcavities," Appl. Phys. Lett. **90**, 051108 (2007).
9. A. Polman, "Erbium implanted thin film photonic materials," J. Appl. Phys. **82**, 1–39 (1997).
10. H. Park, A. Fang, S. Kodama, and J. Bowers, "Hybrid silicon evanescent laser fabricated with a silicon waveguide and III-V offset quantum well," Opt. Express **13**, 9460–9464 (2005).
11. E. H. Sargent, "Infrared quantum dots," Adv. Mater. (Weinheim, Ger.) **17**, 515–522 (2004).

12. J. S. Steckel, S. Coe-Sullivan, V. Bulović, and M. G. Bawendi, "1.3 μm to 1.55 μm Tunable electroluminescence from PbSe quantum dots embedded within an organic device," Adv. Mater. (Weinheim, Ger.) **15**, 1862–1866 (2003).

13. R. H. Hadfield, "Single-photon detectors for optical quantum information applications," Nat. Photonics **3**, 696–705 (2009).

14. I. Fushman, D. Englund, and J. Vučković, "Coupling of PbS quantum dots to photonic crystal cavities at room temperature," Appl. Phys. Lett. **87**, 241102 (2005).

15. Z. Wu, Z. Mi, P. Bhattacharya, T. Zhu, and J. Xu, "Enhanced spontaneous emission at 1.55 mu m from colloidal PbSe quantum dots in a Si photonic crystal microcavity," Appl. Phys. Lett. **90**, 171105 (2007).

16. A. G. Pattantyus-Abraham, H. Qiao, J. Shan, K. A. Abel, T.-S. Wang, F. C. J. M. van Veggel, and J. F. Young, "Site-selective optical coupling of PbSe nanocrystals to Si-based photonic crystal microcavities," Nano Lett. **9**, 2849 (2009).

17. R. Bose, J. Gao, J. F. McMillan, A. D. Williams, and C. W. Wong, "Cryogenic spectroscopy of ultra-low density colloidal lead chalcogenide quantum dots on chip-scale optical cavities towards single quantum dot near-infrared cavity QED," Opt. Express **17**, 22474–22483 (2009).

18. M. T. Rakher, R. Bose, C. W. Wong, and K. Srinivasan, "Spectroscopy of 1.55 μm PbS quantum dots on Si photonic crystal cavities with a fiber taper waveguide," Appl. Phys. Lett. **96**, 161108 (2010).

19. Purchased from Evident Technologies and identified in this paper to foster understanding, without implying recommendation or endorsement by NIST.

20. F. Le Kien, S. Dutta Gupta, V. I. Balykin, and K. Hakuta, "Spontaneous emission of a cesium atom near a nanofiber: Efficient coupling of light to guided modes," Phys. Rev. A **72**, 032509 (2005).

21. M. Davanço and K. Srinivasan, "Efficient spectroscopy of single embedded emitters using optical fiber taper waveguides," Opt. Express **17**, 10542–10563 (2009).

22. K. Nayak, P. Melentiev, M. Morinaga, F. Kien, V. Balykin, and K. Hakuta, "Optical nanofiber as an efficient tool for manipulating and probing atomic fluorescence," Opt. Express **15**, 5431–5438 (2007).

23. M. Gregor, A. Kuhlicke, and O. Benson, "Soft-landing and optical characterization of a preselected single fluorescent particle on a tapered optical fiber," Opt. Express **17**, 24234–24243 (2009).

24. E. Vetsch, D. Reitz, G. Sagué, R. Schmidt, S. T. Dawkins, and A. Rauschenbeutel, "Optical interface created by laser-cooled atoms trapped in the evanescent field surrounding an optical nanofiber," Phys. Rev. Lett. **104**, 203603 (2010).

25. L. Turyanska, A. Patanè, M. Henini, B. Hennequin, and N. R. Thomas, "Temperature dependence of the photoluminescence emission from thiol-capped PbS quantum dots," Appl. Phys. Lett. **90**, 101913 (2007).

26. C. B. Layne, W. H. Lowdermilk, and M. J. Weber, "Multiphonon relaxation of rare-earth ions in oxide glasses," Phys. Rev. B **16**, 10–20 (1977).

27. R. Bose, J. F. McMillan, J. Gao, K. M. Rickey, C. J. Chen, D. V. Talapin, C. B. Murray, and C. W. Wong, "Temperature-tuning of near-infrared monodisperse quantum dot solids at 1.5 μm for controllable Förster energy transfer," Nano Lett. **8**, 2006–2011 (2008).

28. M. T. Rakher, L. Ma, O. Slattery, X. Tang, and K. Srinivasan, "Quantum transduction of telecommunications-band single photons from a quantum dot by frequency upconversion," Nat. Photonics **4**, 786–791 (2010).

29. I. Chung and M. G. Bawendi, "Relationship between single quantum-dot intermittency and fluorescence intensity decays from collections of dots," Phys. Rev. B **70**, 165304 (2004).

30. J. M. Pietryga, D. J. Werder, D. J. Williams, J. L. Casson, R. D. Schaller, V. I. Klimov, and J. A. Hollingsworth, "Utilizing the lability of lead selenide to produce heterostructured nanocrystals with bright, stable infrared emission," J. Am. Chem. Soc. **130**, 4879–4885 (2008).

31. M. J. Stevens, R. H. Hadfield, R. E. Schwall, S. W. Nam, R. P. Mirin, and J. A. Gupta, "Fast lifetime measurements of infrared emitters using a low-jitter superconducting single-photon detector," Appl. Phys. Lett. **89**, 031109 (2006).

1. Introduction

Lead-salt colloidal quantum dots (QDs) [1] such as PbS QDs are interesting active emitters due to the fact that they can be integrated with high quality, Si-based nanophotonic devices designed to operate near 1550 nm [2, 3]. These devices can potentially be used for applications such as ultra-low threshold lasers [4] as well as fundamental studies of light-matter interaction [5]. While significant strides along these lines have been made with self-assembled InAs QDs embedded in GaAs-based devices [6, 7], the optical quality factors (Qs) obtained are usually an order of magnitude lower [8] than what can be achieved in Si, SiO$_2$, or SiN [2]. In addition, the fabrication of electronic and micromechanical systems in Si-based materials is much more mature than in GaAs. Thus, the introduction of an active emitter with Si-based optical micro-

cavities and waveguides is a very active field of research [9, 10]. In contrast to InAs quantum dots, PbS QDs have longer radiative lifetimes by 2 to 3 orders of magnitude [11] and reduced quantum efficiencies by 1 to 2 orders of magnitude when dried [12], yielding a photon emission rate that is as much as five orders of magnitude worse. Combined with the challenges of single-photon detection in the near-infrared [13], performing spectroscopic measurements of low densities of PbS QDs can be difficult and photon collection efficiencies must be as high as possible.

Previous work [14, 15, 16, 17] with lead-salt QDs on microcavities has focused on using free-space optics and microscope objectives to collect emission, but this is limited by the planar geometry of the microcavities. Recently, it was shown that coupling to photonic crystal cavities through a fiber taper waveguide is an efficient method to extract emitted photons [18]. In addition, it was demonstrated that the QDs did not degrade the Q of the cavity up to $Q \approx 3 \times 10^4$. Here, we present further spectroscopic techniques for PbS QDs based upon efficient collection using a fiber taper waveguide (FTW) [3]. In particular, we perform cryogenic photoluminescence (PL) studies of low-densities of QDs dried directly onto an FTW, enabling efficient measurement in a range of environmental conditions. Also, we demonstrate PL and time-resolved PL measurements of QDs dried onto Si microdisk cavities and show that Qs up to 10^5 are unaffected by the QDs. As discussed in the last section of this letter, single PbS QD measurements, like those performed on InAs QDs, will be quite challenging due to the aforementioned detection difficulties and use of the techniques described here will be necessary to make such experiments more feasible.

2. Experimental Setup

The PbS QDs used here are chemically synthesized and stored in a solution of chloroform [19]. Per the manufacturer's specification in solution, these QDs are 5.3 nm $\pm$ 0.5 nm in diameter and have strong optical absorption from 400 nm to 1400 nm. The peak in the emission spectrum in solution is expected near 1450 nm with a width of 150 nm. Experiments are performed using a FTW, which is a single mode optical fiber whose diameter has been adiabatically reduced from 125 μm to $\approx$ 1 μm over a length of 10 mm by heating with a hydrogen torch. Typical losses due to fabrication are less than 0.5 dB. Light propagating through the FTW is used to evanescently excite photoluminescence (PL) from PbS QDs or to probe cavity resonances in Si microdisk structures. Because the FTW begins and terminates as single mode fiber, a variety of tunable laser sources can be easily introduced with a wavelength division multiplexer into the setup as shown in Fig. 1. Each source is required for a different measurement. The 960 nm to 996 nm laser is used to generate excitons far above the photoluminescence at 1500 nm, enabling measurement of the complete emission spectrum. The 1270 nm to 1330 nm laser is used for both CW excitation and pulsed excitation for time-resolved measurements. The 1520 nm to 1630 nm laser is used to measure microdisk cavity resonances in transmission near the emission band of the QDs.

After variable optical attenuation, the sources are introduced through fiber feedthroughs into one of two setups. The first is a liquid He flow cryostat for measurements of PbS QDs on FTWs as a function of temperature, while the second is a N_2-rich room temperature enclosure for measurements of PbS QDs dried onto optical cavities. Temperature measurements are performed in the cryostat using a silicon diode attached adjacent to the copper mount holding the FTW. The FTW is controlled within the room temperature enclosure with high resolution (50 nm minimum step size) stages to enable accurate positioning with respect to microdisk cavities. For transmission measurements, the signal is measured directly with an InGaAs photodiode. For PL measurements, the signal is measured using a monochromator with a liquid-nitrogen-cooled InGaAs array or an InGaAs/InGaP single photon counting avalanche photodiode (APD).
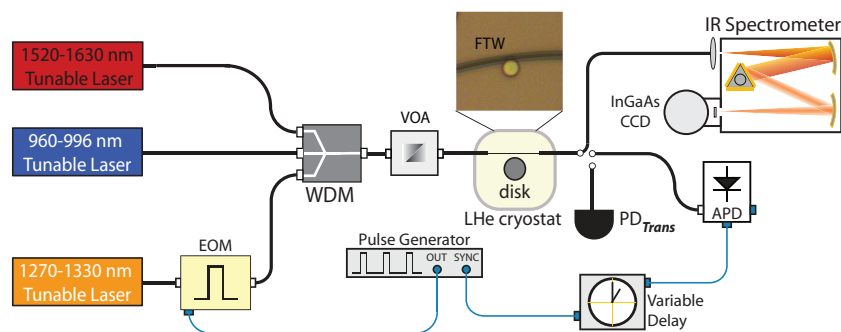
Fig. 1. Experimental setup composed of tunable-wavelength laser sources (980 nm, 1310 nm, and 1550 nm), electro-optic intensity modulator (EOM), wavelength division multiplexer (WDM), variable optical attenuator (VOA), fiber taper waveguide (FTW), cryostat, timing electronics, and measurement devices (spectrometer, photodiode (PD), and InGaAs/InGaP single photon counting avalanche photodiode (APD)).

The pulsed source near 1300 nm required for time-resolved measurements is created using an electro-optic intensity modulator driven by a pulse generator. These instruments combine to create wavelength-tunable (1300 nm to 1320 nm) 22.8 fJ, 2.1 ns pulses at a user-defined repetition rate of 1 KHz to 1 MHz with an on/off extinction ratio of 28.1 dB. It is important to note that the EOM-based pulsed excitation offers substantial flexibility in repetition rate, wavelength, and pulse length compared to most pulsed laser systems. Using a faster pulse generator it would be possible to create pulses as short as 100 ps, making future Purcell effect measurements possible. Because the APD must run in a gated-detection mode, the detection gate is synchronized to the arrival of the optical pulse with a delay generator triggered by the pulse generator as shown in Fig. 1. Time-resolved measurements are accomplished by changing the delay of the APD gating with respect to the arrival of the PL pulse and integrating the counts for a specified time. If the expected decay times were shorter than the width of the APD gate (100 ns maximum), the measurement could be performed in a multi-channel way using a standard time-correlated counting board.

3. Cryogenic and Time-resolved Measurements of PbS QDs dried on FTW

In the first set of measurements, PbS QDs in chloroform solution are diluted to a concentration of 0.5 mg/mL. Then, $\approx$10 μL drops are dried on a glass slide overlayed with the FTW, resulting in a low density ($\approx$ 1000 μm^{-2} as measured by scanning electron microscopy) drying onto the FTW. Previous theoretical [20, 21] and experimental work [22, 23, 24] has shown that FTWs can be efficient channels for the collection of spontaneous emission from nearby, optically-active sources such as atoms, ions, or QDs. In fact, it was shown theoretically [20] that an optimally-sized FTW of diameter $\approx \lambda/4$ could collect approximately 28 % of the total light from a nearby emitter. In the experiments here, the FTW is used both for efficient evanescent excitation and collection of subsequent PL. The FTW is tapered to a nearly-optimal diameter of $\approx$450 nm, see Fig. 2a, to optimize collection efficiency near 1500 nm while minimizing scattering loss. For the FTW shown in Fig. 2a, the loss induced by the tapering was $\approx$5 dB, much more than for a diameter of 1 μm (0.5 dB), and is due to a breakdown of adiabaticity at these small length scales. Given the areal density and the size of the FTW, the total number of QDs that could interact with the propagating optical mode was $\approx 10^6$. The FTW with PbS QDs is loaded into the He-flow cryostat for PL measurements at 293 K, 185 K, and 40 K. PL spectroscopy is performed by exciting the PbS QDs at 980 nm or 1310 nm and measuring the
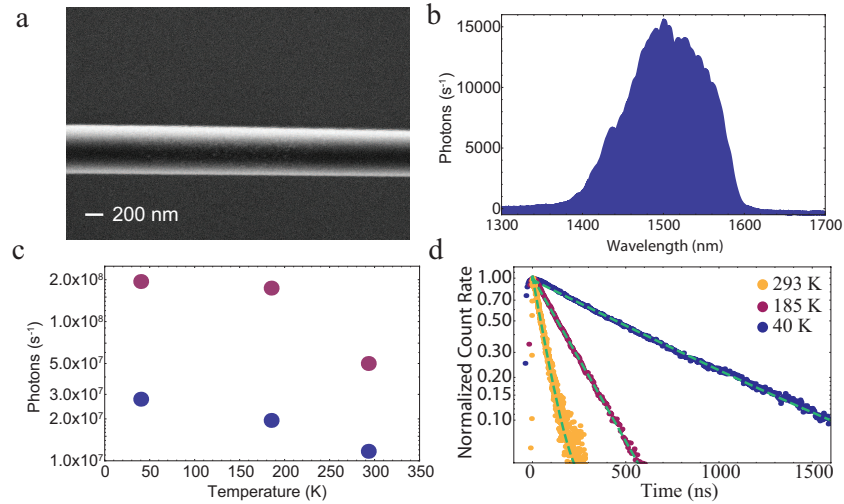
Fig. 2. (a) Scanning electron microscope image of 450 nm diameter fiber taper waveguide with PbS QDs dried on surface (not visible). (b) Spectrum (60 s integration time) of QD PL at 40 K under 6.7 mW of 980 nm excitation. (c) Comparison of total PL counts ($\lambda >$ 1400 nm) under 1 μW (blue) and 10 μW (maroon) 1310 nm excitation at 40 K, 185 K, and 293 K. Errors are contained within the point size. (d) Time-resolved PL traces taken at 40 K, 185 K, and 293 K with 2.1 ns, 22.8 fJ pulses at 1310 nm with 190 kHz repetition rate. The extracted decay times (errors given by 95 % confidence interval) are 58.9 ns ± 3.7 ns, 189.1 ns ± 4.4 ns, and 657 ns ± 10 ns for 293 K, 185 K, and 40 K respectively.

emitted photons with the InGaAs array after spectral dispersion by a monochromator as shown in Fig. 1. A complete 40 K PL spectrum excited by 6.7 mW at 980 nm is shown in Fig. 2b and shows the center of the emission near 1500 nm with a width $\approx$ 175 nm. For comparison at different temperatures, the total collected PL with $\lambda >$ 1400 nm excited by 1 μW (blue) and 10 μW (maroon) at 1310 nm is shown in Fig. 2c for temperatures of 40 K, 185 K, and 293 K. The data clearly show increasing PL count rates for decreasing temperatures. Along with the increase in count rates, the center wavelength was measured to shift slightly to longer wavelengths with decreasing temperature, an effect that has been previously measured for the PbS QDs [25], and serves to verify the temperature assignments.

To further investigate the dynamics of photoluminescence in these QDs at different temperatures, APDs used in conjunction with 190 kHz pulsed excitation at 1310 nm (see Fig. 1) enabled measurement of the excited state lifetime as shown for each temperature in Fig. 2d, where photon counts for $\lambda >$ 1400 nm, are displayed as a function of the delay between the arrival of the optical pulse and the gating of the APD. Each point on the curve was sequentially obtained after 2 s of integration time, followed by a 2 s dark count only measurement for background subtraction. As shown clearly in Fig. 2d, the exponential decay of the excited population changes drastically with temperature resulting in extracted lifetimes (errors given by 95 % confidence interval) of 58.9 ns ± 3.7 ns, 189.1 ns ± 4.4 ns, and 657 ns ± 10 ns for 293 K, 185 K, and 40 K respectively. The simultaneous increase in the measured count rates with an increase in lifetime for decreasing temperatures is strongly indicative of a significant non-radiative decay channel that decreases with temperature. Notably, the data does not fit well to the temperature dependence of multi-phonon relaxation [26] arising from coupling to longitudinal-optical (LO) phonons in PbS at $E_{LO} = 26$ meV [25], which indicates some other form of energy transfer. Such energy transfer effects are common phenomena in other solid-state optical emitters and
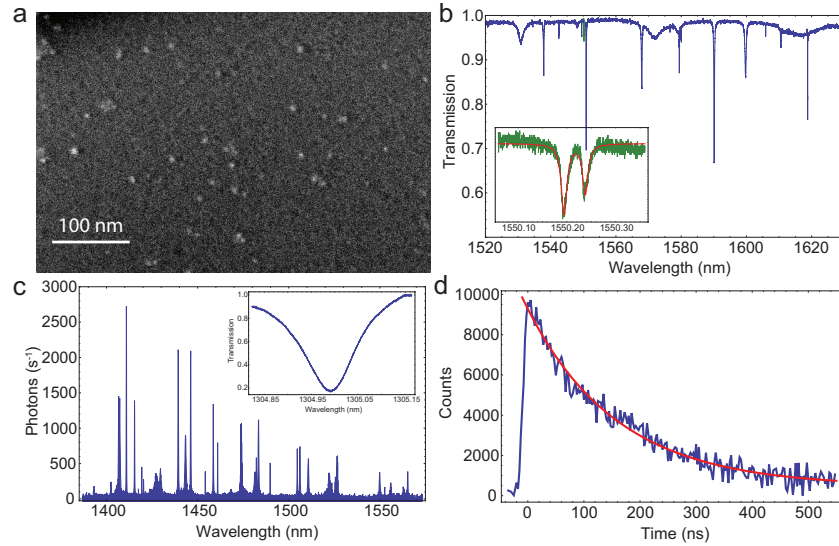
Fig. 3. (a) SEM image of PbS QDs deposited on the surface of a Si microdisk, corresponding to an areal density of $\approx 2000~\mu\text{m}^{-2}$. (b) Transmission measurement of the FTW coupled to a Si microdisk from 1520 nm to 1630 nm, showing several cavity modes. A $Q \approx 1.1 \times 10^5$ doublet is shown in green and enlarged with fit in inset. (c) PL measurement of QD emission collected by the FTW in contact with the microdisk under pulsed excitation at 1304 nm. Inset: Transmission spectrum of the pump mode at 1304 nm with $Q \approx 9 \times 10^3$ and $\Delta T = 0.92 \pm 0.02$. (d) Time-resolved PL decay trace measured with the InGaAs/InGaP APD.

somewhat limits their utility at room-temperature. Specifically, fundamental light-matter studies need to be performed at temperatures with the best possible quantum coherence.

4. Time-resolved Measurements of PbS QDs on Si Microdisks

To investigate coupling to cavities, a low density of PbS QDs were spun directly onto a wafer containing 4.5 μm diameter Si microdisk cavities. These cavities were fabricated using standard silicon-on-insulator processing with a 250 nm thick device layer. An SEM of the surface of one such microdisk is shown in Fig. 3a after PbS QD spin, resulting in a QD density of approximately 2000 μm^{-2} with approximately 10^4 within the cavity mode volume. In order to determine the optical quality factors, the FTW was positioned in the near-field of the cavities to enable efficient, resonant interaction with light propagating down the fiber. As in Fig. 1, a tunable 1500 nm band laser was swept in wavelength, coupled to the microdisk via the FTW, and measured with a low-noise InGaAs photodiode. The resulting transmission as a function of wavelength from 1520 nm to 1630 nm is shown in Fig. 3b, where several sharp modes are clearly visible. For this particular cavity, Qs ranged from 5×10^3 to 1.1×10^5 (see inset of Fig. 3b). The best measured Qs (device not shown) were 2×10^5 and were likely limited by sidewall roughness induced in the etching procedure. Errors in fitted Q values arise from fitting the data and are smaller than the last given digit. Similar to [18], microdisks were measured before and after QD deposition to determine if there was any effect on the Q factor. Up to $Q \approx 2 \times 10^5$, there was no measurable Q degradation caused by the presence of the QDs.

Because of the rich mode structure of the disk and the optical properties of Si, high-Q modes can be measured into the absorption band of the QDs and down to 1200 nm. One such mode

is shown in transmission in the inset of Fig.3c with $Q \approx 9 \times 10^3$. The FTW enables efficient coupling to this mode with coupling depth $\Delta T = 0.92 \pm 0.02$, just short of critical coupling, ensuring almost complete transfer of power. By pumping on this mode, only QDs on the circumference of the disk are excited by the circulating pump. The 1300 nm tunable laser combined with the EOM enable cavity-resonant pulsed excitation. Using 2.1 ns pulses at 1304 nm (resonant with the mode) with 1 MHz repetition rate, the QDs emit a PL signal under 79 nW of average power as shown in the spectrum in Fig. 3c. The significant reduction in average power required to obtain a bright PL spectrum is due to the buildup of power in the cavity mode. In the spectrum, the modes of the microdisk in the emission band are clearly visible and dress the broad PL signal of the QDs. The significant difference between the spectrum in Fig. 3c compared to that of bulk QD emission (see Fig. 2b) verifies that the majority of the collected PL is emitted by QDs into the cavity modes at the circumference rather than directly into the FTW from QDs near to the center of the disk. Incorporation of the gated APD and requisite timing electronics enables a time-resolved measurement of the PL decay as shown in Fig. 3d. The lifetime extracted from this room-temperature measurement is 160 ns $\pm$ 20 ns. This lifetime is longer than that measured for the QDs dried directly on the FTW at room-temperature, but is of the same order of magnitude. We measure markedly different room temperature excited state lifetimes for different samples which implies strong density-dependent or environmentally-dependent decay dynamics such as Förster resonant energy transfer (FRET) [27]. These effects need to be investigated further and will be the focus of future work.

5. Discussion and Conclusion

We have demonstrated techniques for efficient collection of photons emitted by PbS QDs in the 1.5 μm band using FTWs in different environments as well as on microdisk cavities. Using these collection strategies, it is an important exercise to consider if it is experimentally feasible to detect the single photon emission from a single PbS QD in a lifetime measurement and in a Hanbury-Brown and Twiss setup, much like what is done with InAs QDs. In the collection geometries presented here, the fraction of spontaneous emission collected in the measurement mode should be on the order of 1 % to 28 % [20], neglecting any substantial Purcell enhancement. Coupled with assumed radiative lifetimes as long as 700 ns, photoluminescence photon rates from a single PbS QD should reach as high as $\approx 2 \times 10^5$ s^{-1} under saturated continuous wave excitation if the radiative efficiency at low temperature approaches unity. However, these seemingly high count rates are mitigated by the difficulties of single photon detection in the near-infrared [13]. In particular, for the InGaAs APD used in our experiments, the optimum detection parameters for a single-channel lifetime measurement like that found in Fig. 2d and Fig. 3d are a 20 % detection efficiency, 100 ns gate width, and 10 μs dead time for a 1 MHz trigger rate. These settings have a dark count rate of $\approx 1.7 \times 10^3$ s^{-1}, yielding a signal to noise ratio of $\approx$35.4 Hz$^{-1/2}$. Experimentally, this means that the excited-state decay will be observed with a dynamic range of 35.4 if each temporal point is integrated for 1 s, corresponding to a measurable decay over a time period of $\approx$ 3.5 times the decay constant. Compared to an upconversion, multi-channel Si APD measurement for InAs QDs, the dynamic range is approximately a factor of 30 times worse [28].

More important than a lifetime measurement is that of the second order intensity correlation $g^2(\tau)$, where

$$g^{(2)}(\tau) = \frac{\langle a^\dagger(t)a^\dagger(t+\tau)a(t+\tau)a(t)\rangle}{\langle a^\dagger(t+\tau)a(t+\tau)\rangle\langle a^\dagger(t)a(t)\rangle}, \qquad (1)$$

and a ($a^\dagger$) is the photon annihilation (creation) operator, which yields information about the non-classicality of the emitted photon stream. Specifically, a measured value of $g^{(2)}(0) < 0.5$

proves that the field is dominantly composed of single photons. Using a standard Hanbury-Brown and Twiss setup, a minimum measurable $g^{(2)}(0)$ value for a PbS QD would be ≈ 0.60 using a 10 % detection efficiency, 2.5 ns gate width, and 10 μs dead time for a 1 MHz trigger rate. While this is a reasonably low value (proving the field is non-classical but not single photon), the signal to noise under these measurement conditions is only ≈ 0.011 Hz$^{-1/2}$, requiring more than two hours of integration time to achieve unity signal to noise. A signal to noise of ≈ 0.16 Hz$^{-1/2}$ could be obtained by increasing the gate width to 50 ns, but the minimum measurable $g^{(2)}(0)$ under these conditions is ≈ 0.81. In summary, under the best possible collection conditions and assuming perfect radiative efficiency, it is not possible to measure $g^{(2)}(0) < 0.5$ using commercially available detectors. In addition, the assumption of perfect radiative efficiency does not match experimental observation, even at cryogenic temperatures. This could be caused by several factors including blinking [18, 29] and poor radiative efficiency out of solution [12]. Therefore, it appears that single QD measurements at these wavelengths may remain elusive until higher optical quality QDs can be regularly fabricated [30]. However, once these QDs are realized, measurement of single photons will likely require advanced detector technologies such as frequency upconversion [28] or superconducting single photon detectors [31]. Nonetheless, the efficient and flexible measurement techniques presented here will be of great use towards the development of PbS QDs as active emitters coupled to high-quality nanophotonic devices in the telecommunications-band.

Acknowledgements